Proteomic profiling of *Plasmodium falciparum* through improved semi-quantitative, two-dimensional gel electrophoresis

Journal:	*Journal of Proteome Research*
Manuscript ID:	pr-2009-009244.R1
Manuscript Type:	Article
Date Submitted by the Author:	
Complete List of Authors:	Smit, Salome; University of Pretoria, Biochemistry Stoychev, Stoyan; CSIR, Biosciences Louw, Abraham; University of Pretoria, Biochemistry Birkholtz, Lyn-Marie; University of Pretoria, Biochemistry

Proteomic profiling of *Plasmodium falciparum* through improved, semi-quantitative two-dimensional gel electrophoresis

Salome Smit[1], Stoyan Stoychev[2], Abraham I Louw[1], Lyn-Marie Birkholtz[1]*

[1]Department of Biochemistry, Faculty of Natural and Agricultural Sciences, University of Pretoria, Pretoria, 0002, South Africa,

Telephone +27 12 420 2479, Fax +27 12 362 5302

[2]CSIR Biosciences, Pretoria, 0001, South Africa

RECEIVED DATE:

TITLE RUNNING HEAD: Proteomic profiling of Plasmodial proteins

* Corresponding author: Prof Lyn-Marie Birkholtz, Department of Biochemistry, Faculty of Natural and Agricultural Sciences, University of Pretoria, Pretoria, South Africa, 0002

Telephone +27 12 420 2479, Fax +27 12 362 5302, email: lbirkholtz@up.ac.za

ABSTRACT

Two-dimensional gel electrophoresis (2-DE) is one of the most commonly used technologies to obtain a snapshot of the proteome at any specific time. However, its application to study the Plasmodial (malaria parasite) proteome is still limited due to inefficient extraction and detection methods and the extraordinarily large size of some proteins. Here, we report an optimized protein extraction method, the most appropriate methods for Plasmodial protein quantification and 2-DE detection and finally protein identification by mass spectrometry (MS). Linear detection of Plasmodial proteins in a optimized lysis buffer was only possible with the 2-D Quant kit and of the four stains investigated, Flamingo Pink was superior regarding sensitivity, linearity and had excellent MS-compatibility. 2-DE analyses of the Plasmodial proteome using this methodology, resulted in the reliable detection of 349 spots and a 95% success rate in MS/MS identification. Subsequent application to the analyses of the Plasmodial ring and trophozoite proteomes ultimately resulted in the identification of 125 protein spots, which constituted 57 and 49 proteins from the Plasmodial ring and trophozoite stages, respectively. This study additionally highlights the presence of various isoforms within the Plasmodial proteome, which is of significant biological importance within the Plasmodial parasite during development in the intra-erythrocytic developmental cycle.

KEYWORDS: 2-D gel electrophoresis, malaria, fluorescent dyes, proteome, isoforms

INTRODUCTION

Global efforts to eradicate malaria in Third World countries are hampered by various factors including global climate changes, increasing migration behavior, failing health care systems, absence of a licensed vaccine and most disturbingly, the rapid development and dispersal of the respective drug- and insecticide-resistant forms of the malaria parasite and the mosquito vector. About 40% of the world's population in 107 countries live under the constant risk of malaria infection and more than 80% of malaria-associated deaths in the world occur in Africa south of the Sahara. Currently, only one drug, Artemisinin, is still effective against the malaria parasite but the first signs of drug resistance has now emerged at the Thai-Cambodian border[1]. This raises serious concerns and underscores the urgency for innovative strategies to discover new and robust antimalarial drugs as well as new targets to combat the disease. The latter can be expedited by the inclusion of techniques such as functional genomics in drug-discovery pipelines[2].

The *Plasmodium* parasite has complex life cycles in both the human host and the mosquito vector. Pathogenesis is displayed during the 48 hour schizogony of the parasite in human erythrocytes (intra-erythrocytic developmental cycle, IDC), where parasites mature from ring to trophozoite stages to the ultimate production of daughter merozoites from schizonts. This asexual replication cycle is tightly controlled in *P. falciparum* with a unique cascade of gene regulation resulting in the 'just-in-time' production of transcripts coordinated with expression of genes involved in related biological processes[3]. Therefore, in the majority of cases, proteins are produced from their respective transcripts without delay[3, 4].

The resultant Plasmodial proteome is multifaceted and stage-specific, indicating a high degree of

specialization at the molecular level to support the biological and metabolic changes associated with each of the life cycle changes[5, 6]. Post-translational modifications are employed as a mechanism to regulate protein activity during the parasite's life cycle[7] and certain proteins are predicted to act as controlling nodes that are highly interconnected to other nodes and thus results in a highly specialized interactome[2]. These enticing properties motivate studies focused on in-depth characterization of the Plasmodial proteome including regulatory mechanisms and the ability to respond to external perturbations. Analysis of the schizont stage proteome reinforced the notion that both post-transcriptional and post-translational mechanisms are involved in the regulation of protein expression in *P. falciparum*[8].

Due to the >80% AT-richness of the Plasmodial genome[9], the resultant Plasmodial proteome contains proteins in which long hydrophobic stretches and amino acid repeats (notably consisting of lysine and asparagine) are found. Moreover, the proteins from this parasite are comparatively large, non-homologous and highly charged with multiple isoforms within the parasite[10]. These properties have confounded analyses of the Plasmodial proteome, including the recombinant expression of Plasmodial proteins[11, 12]. Few studies attempted to describe the Plasmodial proteome, which is predicted to have about 5300 proteins of which ~60% are hypothetical and un-annotated[8, 13, 14].

The reported efficacy of two-dimensional gel electrophoresis (2-DE) to analyze the Plasmodial proteome is relatively poor since only a low number of protein spots could be detected with various protocols and stains[13-17]. The highest number of spots detected to date on Plasmodial 2-DE gels with silver staining is only 239[15] and recently, a total of 345 spots were detected for 4 time points in the Plasmodial schizont stage using two-dimensional differential gel electrophoresis (2-D DIGE)[8], of which only 54 protein spots were identified. This clearly illustrates the need for an optimized protocol including extraction, quantification and detection methods. This study details such an optimized 2-DE

protocol, which was applied to the analysis of the Plasmodial proteome in the ring and trophozoite stages. This study first optimized established methodology with regard to protein extraction, quantification, detection and finally MS identification. Once the protocol was established, it was subsequently applied to the analyses of the soluble Plasmodial proteome, resulting in the detection of 349 spots using the fluorescent stain, Flamingo Pink, with a 95% success rate achieved in the mass spectrometry (MS) identification of a subset of these proteins, far exceeding previously reported Plasmodial protein identification success rates of 50-79%[13, 14]. After the successful establishment of the optimized 2-DE protocol, this methodology was applied to the Plasmodial ring and trophozoite proteomes for which a total of 125 protein spots were identified. Several protein isoforms were also identified in the two Plasmodial life-stages which has biological significance for the Plasmodial parasite.

EXPERIMENTAL SECTION

Culturing of parasites

P. falciparum 3D7 (*Pf*3D7) parasites were maintained *in vitro* in human O^+ erythrocytes in RPMI 1640 media (Sigma) with 0.5% (w/v) Albumax II (Gibco)[18]. Parasites were synchronized (~98% morphological synchronicity) with sorbitol treatment for three consecutive generations. Thirty milliliters of *Pf*3D7 parasite cultures at 8% parasitemia and 5% hematocrit were used per gel to establish the proteomics methodology. Saponin was added to a final concentration of 0.01% (v/v) followed by incubation on ice for 5 min to lyse the erythrocytes. Parasites were collected by centrifugation at 2500 g for 15 min at room temperature, and washed in PBS at 16 000 g for 1 min at 4□C. This step was repeated at least four times until the supernatant was clear instead of three times as previously reported[7]. The parasite pellet was stored at –80□C. For analyses of proteomes of different developmental states of the parasites, parasites were harvested from 60 ml cultures at 16 hours post invasion (HPI) (late rings) and 20 HPI (early trophozoites).

Protein preparation

Parasite pellets were suspended in 500 µl lysis buffer as described by Nirmalan *et al.* (8 M urea, 2 M thiourea, 2% CHAPS, 0.5% (w/v) fresh DTT and 0.7% (v/v) ampholytes)[7]. Samples were pulsed-sonicated on a Virsonic sonifier with microtip for 20 sec with alternating pulsing (1 sec pulse, 1 sec rest) at 3 W output with 1 min cooling steps on ice (to prevent foaming and carbamylation) and repeated 6 more times. Sonication was followed by centrifugation at 16 000 g for 60 min at 4˚C, after which the protein-containing supernatant was used in subsequent 2-DE.

Protein quantification

Four different protein quantification methods were tested on the samples obtained using two BSA standard curves in each of the methods: firstly, BSA in 0.9% saline, and secondly, BSA in the Plasmodial optimized lysis buffer, each containing the same amount of protein for analysis. The Quick Start™ Bradford dye method (BioRad) was used for protein determination at an absorbance of 595 nm[19]. The Lowry method used a reaction mixture containing solution A (2% (w/v) $NaCO_3$, 2% (w/v) NaOH, 10% (w/v) Na_2CO_3), solution B (2% (w/v) $CuSO_4.5H_2O$), and solution C (0.5% (w/v) potassium tartrate). Two hundred microlitres of the reaction mixture was added to each protein sample, mixed and incubated for 15 min at room temperature. Six hundred microlitres of Folin Ciocalteau reagent (1:10, FC reagent and H_2O) were added and incubated at room temperature for 45 min in the dark. Absorbance was measured at 660 nm[20]. Lastly, two commercial protein concentration determination kits were used according to the manufacturer's instructions and included the Micro BCA™ Protein assay kit (Pierce) and the 2-D Quant Kit (GE Healthcare).

SDS-PAGE gels

Low molecular weight markers (GE Healthcare) were diluted in reducing buffer (0.06 M Tris-HCl, 2% (w/v) SDS, 0.1% (v/v) glycerol, 0.05% (v/v) β-mercaptoethanol and 0.025% (v/v) bromophenol blue, pH 6.8), to provide a concentration range from 100 ng to 0.6 ng protein. Equal amounts of markers were loaded onto four different 12.5% SDS-PAGE gels and the gels were subsequently stained with

either Colloidal Coomassie, silver, SYPRO Ruby (Molecular Probes) or Flamingo Pink (Bio-Rad) stains. The gels were scanned on a Versadoc 3000 and analyzed using the Quantity One Program (Bio-Rad). The Rf values and the intensities of each band were compared, and used to determine the limit of detection and linearity.

Two dimensional gel electrophoresis (2-DE)

For 2-DE, the protein concentration was determined with the 2-D Quant kit. Two hundred micrograms of protein in rehydration buffer (8 M urea, 2 M thiourea, 2% (w/v) CHAPS). 0.5% (w/v) DTT and 0.7% (v/v) IPG Buffer (pH 3-10 Linear) was applied to a 13 cm IPG, pH 3-10 L strip. First dimensional isoelectric focusing was performed on an Ettan IPGphore Isoelectric Focusing Unit (GE Healthcare), and commenced with a 10 hour active rehydration step. Isoelectric focusing time followed an alternating gradient and step-and-hold protocol and was always allowed to proceed to a total of 18 500 Volt-hours, that completed within 15 hours. IPG strips were equilibrated for 10 min each in SDS equilibration buffer (50 mM Tris-HCl, pH 6.8, 6 M urea, 30% (v/v) glycerol, 2% (w/v) SDS, 0.002% bromophenol blue) containing 2% DTT, and then incubated in 2.5% iodoacetamide. Finally, the strip was placed in SDS electrophoresis running buffer (0.25 M Tris-HCl, pH 8.3, 0.1% SDS, 192 mM glycine) for 10 min as a final equilibration step. Second dimensional separation was performed by placing the IPG strips on top of the 10% SDS PAGE gel (Hoefer SE 600), covered with 1% agarose dissolved in SDS electrophoresis running buffer. Separation was performed at 80 V at 20°C until the bromophenol blue front reached the bottom of the gel. The gels were then fixed in the appropriate fixing solution for each specific stain (see below). For the method optimization protocol, gel image analysis was performed using PD Quest 7.1.1 (Bio-Rad). All 8 gels were filtered using the Filter Wizard. Spot detection was performed on the gels by automated spot detection. The display of the gels stained with SYPRO Ruby and Flamingo Pink was inverted for easier comparisons with the gels stained with CCB and silver. Additional manual settings for spot detection were sensitivity (2.22), size scale (5) and min peak (1244). For proteomic analyses of the different developmental stages of *P. falciparum*, 400 µg

protein was applied to 18 cm IPG strips for separation and subsequently stained with Flamingo Pink and scanned using the Versadoc 3000 as described below. PD Quest 7.1.1 was used to identify the number of spots on each of the gels that were done for the ring and trophozoite 2-DE proteomes (8 gels for each stage). First, all images were cropped to the same dimensions (1.59 Mb, 933 x 893 pixels, 303.7 x 290.7 mm) and filtered using the salt setting (light spots on dark background) of the Filter Wizard. The Spot Detection Wizard was used to automatically detect spots on the selected master image by manual identification of a small spot, faint spot and large spot. Additional settings for spot detection were manually selected for sensitivity (5.31 for rings and 4.35 for trophozoites), size scale 5.0 (both), min peak (808 for rings and 4712 for trophozoites). After automated matching of all the gels, every spot were manually verified to determine correctness of matching. The master image contained 369 spots for the ring stage proteome with a match rate of 98%, and the trophozoite master image contained 450 spots with a match rate of 96%.

Flamingo Pink staining of 2-DE gels

Gels were fixed overnight in 40% (v/v) ethanol, 10% (v/v) acetic acid, and subsequently in 200 ml Flamingo Pink working solution and incubated with gentle agitation in the dark for 24 hours, to increase the sensitivity of the stain. The gels were washed in 0.1% (w/v) Tween-20 for 30 min to reduce background. Finally the gels were rinsed in MilliQ water twice before scanning on the Versadoc 3000. All gels were stored in Flamingo Pink at 4ºC until use for MS.

Silver staining of 2-DE gels

Gels were fixed in 45% (v/v) methanol, 5% (v/v) acetic acid overnight, followed by sensitizing for 2 min in 0.02% (w/v) sodium thiosulfate, and rinsing with MilliQ water twice. 200 ml ice cold 0.1% (w/v) silver nitrate was added and incubated at 4°C for 30 min, rinsed twice with MilliQ water and developed in fresh 2% (w/v) sodium carbonate with 0.04% (v/v) formaldehyde. Development was stopped by adding 1% (v/v) acetic acid. All gels were stored in 1% (v/v) acetic acid at 4ºC in airtight containers

until use for MS.

SYPRO Ruby staining of 2-DE gels

Gels were fixed in 10% (v/v) methanol, 7% (v/v) acetic acid overnight. The fixing solution was replaced with 200 ml SYPRO Ruby stain and incubated with agitation for 24 hours in the dark, to increase sensitivity. After staining, the gels were washed for 60 min with 10% (v/v) methanol, 7% (v/v) acetic acid to reduce fluorescent background. Finally the gels were rinsed twice with MilliQ water before scanning on the Versadoc 3000. Gels were stored in SYPRO Ruby at 4°C until use for MS.

Colloidal Coomasie Blue (CCB) staining of 2-DE gels

Colloidal Coomassie Brilliant Blue G250 stock solution (2% (v/v) phosphoric acid, 10% (w/v) ammoniumsulfate, and 0.1% (v/v) Coomassie Brilliant Blue G250) was diluted (4:1) with methanol just before use. The gels were immersed in the Colloidal Coomassie solution and left shaking overnight. Gels were rinsed with 25% (v/v) methanol, 10% (v/v) acetic acid before destaining with 25% (v/v) methanol, until the background was clear[21]. Gels were then scanned on the Versadoc 3000, and stored in 1% (v/v) acetic acid at 4°C until use for MS.

2-D spot identification by tandem mass spectrometry

For comparative purposes mostly the same 39 spots (154 in total) covering a wide range on the gels as well as low molecular weight markers were cut from each of the 4 differently stained gels, dried and stored at -20°C. The silver stained samples were first destained with potassium ferricyanide and sodium thiosulfate to remove the silver before proceeding to wash steps[22]. All gel pieces was cut into smaller cubes and washed twice with water followed by 50% (v/v) acetonitrile for 10 min each. The acetonitrile was replaced with 50 mM ammonium bicarbonate and incubated for 10 min, repeated twice, except for CCB samples, which had an additional wash step to ensure complete removal of the dye. All the gel pieces were then incubated in 100% acetonitrile until they turned white. This was followed by another ammonium bicarbonate, acetonitrile wash step as above, after which the gel pieces were dried *in vacuo*. Gel pieces were digested with 10 ng/µl trypsin at 37°C overnight. Resulting peptides were extracted

twice with 70% acetonitrile for 30 min, and then dried and stored at -20°C. Dried peptides were dissolved in 10% (v/v) acetonitrile, 0.1% (v/v) formic acid and mixed with saturated alpha-cyano-4-hydroxycinnamic acid before being spotted onto a MALDI sample plate. Experiments were performed using Applied Biosystems QSTAR-ELITE, Q-TOF mass spectrometer with oMALDI source installed. Laser pulses were generated using a Nitrogen laser with intensities between 15 and 25 µJ depending on sample concentration and whether single MS or MS/MS experiments were performed. First, single MS spectra were acquired for 15-30 sec. The 50 highest peaks from the MS spectra were automatically selected for MS/MS acquisition. Tandem spectra acquisition lasted 4-8 min depending on sample concentration. Argon was used as cooling gas in Q0 and collision gas in Q2. The collision energy was first optimized using a 9 peptide mixture covering the scan range of 500–3500 Da and then automatically set during MS/MS experiments using the Information Dependent Acquisition (IDA) function of the Analyst QS 2.0 software. The instrument was calibrated externally, in TOF-MS mode, via a two point calibration using the peptides Bradykinin 1-7 and Somatostatin 28 ($[M+H]^+$ = 757.3992 Da and 3147.4710 Da, respectively). Data was submitted in MASCOT (www.matrixscience.com). For the Plasmodial ring and trophozoite proteome analysis, spots of various intensities covering the whole 2-DE range (pI 4-9, and Mr 13-135 kDa) were selected, and subjected to MS/MS as described above. For the ring stage 2-DE proteome analysis 77 spots were selected for MS identification and 63 spots were selected for the trophozoite stage. The normalized intensities of these spots ranged from 58 to a maximum of 9734 with 1963 as the average intensity per spot.

Results and Discussion

Optimization for 2-DE of Plasmodial proteins

The ability of 2-DE to provide a snapshot of the proteome at any particular time, is a distinct advantage for a multistage organism such as *Plasmodium*. The 2-DE technique remains the most widely used for proteomic investigation techniques[23] due to several advantageous properties such as good resolution of abundant proteins as well as information on protein size, quantity and isoforms with post-

translational modifications or different pIs[24]. However, 2-DE gels are biased to the detection of relatively high abundant proteins as well as soluble and mid-range molecular weight proteins[25]. Besides the visual advantages of 2-DE in comparing protein levels, proteins are differentially stained due to their specific chemical and physical properties, which necessitates careful selection of the staining method in terms of its sensitivity, reproducibility, ease of use and cost-effectiveness. Most importantly, the stain should be compatible with downstream applications such as MS. This study describes an improved protocol for the detection and identification of Plasmodial proteins separated by 2-DE, which was then also subsequently applied to identify the proteome of the Plasmodial ring and trophozoites stages.

The analysis of the Plasmodial proteome by 2-DE has been hampered by numerous technical constraints. Plasmodial proteins are notoriously insoluble, comparatively large, non-homologous and highly charged[10] and therefore necessitates the use of optimized lysis buffers to ensure maximal solubility of these proteins for 2-DE. The lysis buffer described by Nirmalan *et al.,* is able to solubilize a large proportion of Plasmodial proteins. In this study, the combination of 5-fold less saponin used, increased washing steps and shorter sonication cycles (with prolonged cooling in between cycles), contributed to the absence of hemoglobin on the 2-DE gels and the detection of proteins in the range of pH 8-9 that was previously cumbersome in Plasmodial 2-DE. The use of this lysis buffer, however precludes the use of traditional methods of protein concentration determination.

A two-pronged approach was used in this study to determine the most effective and reproducible detection and staining method for Plasmodial proteins. Firstly, the effect of the extraction medium on standard protein determination methods was established as well as the sensitivity of staining methods to detect gel-separated molecular weight standards and secondly, for comparative purposes the sensitivity and reproducibility of these staining methods to detect Plasmodial proteins on 2-DE gels. Four different methodologies were evaluated to determine Plasmodial protein concentrations in the lysis buffer used

for the protein extraction. The standard Bradford method as well as the Lowry and BCA methods was found to be incompatible with the lysis buffer, (results not shown). The 2-D Quant kit conversely provided reproducible and comparable data for both the saline (R^2 = 0.9918) and lysis buffer (R^2 = 0.9929) standard curves, most likely due to the quantitative protein precipitation step by which any other interfering substances in the lysis buffer are also removed. Although various Plasmodial proteomic studies have employed the Bradford method[14, 15], the present study confirms recent reports of the reliability of the 2-D Quant method[8, 26].

A second caveat in semi-quantitative proteomics is the sensitivity of the staining method used for the detection of protein spots after 2-DE. The sensitivity, performance, and linear regression constants of four different staining methods were compared in this study with quantitative 1-D analyses of standard molecular weight markers. Four different SDS-PAGE gels were individually stained with Colloidal Coomassie Blue (CCB), MS-compatible silver stain, SYPRO Ruby and Flamingo Pink, and compared by using Quantity One 4.4.1 to determine the detection limits (Table 1, 1-D SDS PAGE MW analysis of stains). SYPRO Ruby and Flamingo Pink achieved similar results, as both were able to detect up to 1 ng of protein and were linear (R^2 = 0.97). CCB was the least sensitive of the four stains with a detection limit of 25 ng and relatively poor linearity (R^2 = 0.89). The MS-compatible silver stain was able to detect a minimum of 10 ng but has a very poor linear range (R^2 = 0.83). The fluorescent stains, SYPRO Ruby and Flamingo Pink, thus seem superior to CCB and silver in both sensitivity and dynamic linear quantification range of standard protein molecular weight markers.

These same stains were subsequently tested on the proteome of Plasmodial proteins after 2-DE. The total Plasmodial trophozoite proteome is predicted to contain 1029 proteins[27, 28] (PlasmoDB 6.0), which spans a wide molecular weight range and pI with different degrees of solubility. Filtering of this dataset to represent the conditions used in this study for 2-DE resulted in 443 Plasmodial trophozoite proteins

that should be detectable on a standard 2-DE gel in the molecular weight range of 10-110 kDa with a pI range of 4-9. Duplicate 2-DE analysis were performed for all 4 stains used (n = 2 per stain and n = 8 in total). The CCB stain performed poor in detection with an average of 126 spots detected, markedly less than any of the other three stains tested (Table 1, 2-DE trophozoite analysis of stains). The MS-compatible silver stain was superior in terms of sensitivity and 420 spots of the Plasmodial trophozoite proteome could be detected (Fig. 1). This represents 95% (420/443) of the expected trophozoite proteome that were detected here. However, the poor linearity and spurious artifacts associated with silver staining of 2-DE could lead to unreliable results when groups of gels with differentially expressed proteins are compared (Table 1)[29].

Fluorescent stains have been developed with seemingly similar sensitivity to silver as well as being MS-compatible, which include the earlier SYPRO Orange and SYPRO Red[30, 31], and the currently commonly used SYPRO Ruby stain[29]. The latter is a fluorescent ruthenium-based stain that binds non-covalently to protein in gels, and is used to stain refractory proteins like glycoproteins and lipoproteins. SYPRO Ruby has been reported to be a photostable end-point stain, with a good linear dynamic range[29, 32] and to be MS compatible[33]. However, SYPRO Ruby was only able to detect 235 Plasmodial protein spots after 2-DE with a MS identification rate of 85% (Table 1). These results are in sharp contrast to those obtained with standard protein molecular weight markers and indicate that SYPRO Ruby is not an appropriate stain to use with Plasmodial proteins. New generation fluorescent stains such as Flamingo Pink are reported to be able to detect proteins across the full range of molecular weights and isoelectric points separated on 2-DE with little gel-to-gel variability[34], good linear dynamic range and MS-compatibility. These properties seem to be supported by the results of this study since 79% (349/443) of the Plasmodial trophozoite proteome were detected on 2-DE as predicted by our calculations.

In order to assess the overall MS-compatibility of the four staining methods, approximately 39 spots

of four individual gels were selected consisting of 33 Plasmodial proteins (Fig. 1, 1-33) and 6 standard molecular weight marker proteins (Fig. 1, marked Mr1 to Mr6), summarized in Table 1 (2-DE trophozoite analysis of stains). Proteins were identified when a significant Mascot score was obtained and further criteria of at least 5 peptides and sequence coverage of at least 10% was achieved (Supplementary Tables 1 A-D). This was done to increase the MS/MS identification confidence. Silver staining resulted in the least number of positive identifications (85%) with MS/MS (Table 1). This low positive identification value was also observed for SYPRO Ruby staining. The most promising results concerning protein identification were obtained with CCB and Flamingo Pink, which both had MS/MS success rates in excess of 90% (CCB had positive identification for 35/37 proteins subjected to MS/MS and Flamingo Pink had positive identification for 37/39 proteins subjected to MS/MS). The MS-compatibility of CCB is well documented[35, 36], but literature evidence for the MS-compatibility of Flamingo Pink is still lacking. However, for the Plasmodial proteins investigated here, Flamingo Pink was superior to the other standard stains regarding its ability to provide excellent MS/MS identification rates (95% success). Moreover, it provides an excellent linear dynamic range ($R^2 = 0.97$) as detected on 1-D SDS PAGE gels with standard molecular weight markers and was able to detect 79% of the predicted 2-DE trophozoite proteome under our experimental conditions. Thus, Flamingo Pink provided high sensitivity to detect proteins on both 2-DE and 1-D gels, as well as good linear dynamic ranges with the added advantage of excellent MS-compatibility. This suggests that Flamingo Pink may the preferable stain as far as Plasmodial proteomics are concerned but this may also be generally true for proteome analyses due to its superior detection and identification of proteins after 2-DE.

2-DE based analyses of the Plasmodial proteome is hampered by contaminating hemoglobin derived products (HDP)[37], possibly as a result of the thiourea/sonication steps during the extraction of Plasmodial proteins, and the resultant destabilization of hemozoin. Typically, these HDPs are observed as an intense smear focused around pI 7-10 with varying molecular weights. The less harsh sonication

steps used in this study combined with extensive wash steps (to remove hemoglobin) and 5-fold less saponin, resulted in discrete spots identified in the 2-DE based Plasmodial proteome described here. Very little background and smearing were observed here compared to other Plasmodial proteome studies[7, 14, 15, 38] enabling the identification of several proteins in the pI 7.5-9 range (Fig. 1, e.g. LDH, G3PDH, Adenylate kinase). Moreover, the protocol used here makes it unnecessary to use additional fractionation steps to remove contaminating high pI fractions[37] or two-step extraction procedures[15]. Furthermore, the use of the 2-D Quant kit provided the only means of protein concentration determination for Plasmodial proteins in the lysis buffer. Finally, Flamingo Pink proved to be superior with regard to sensitivity as far as detection of spots on 2-DE is concerned and provided excellent MS/MS compatibility for Plasmodial proteins.

Application of 2-DE optimized method on the Plasmodial ring and trophozoite stages

The successful establishment of an optimized 2-DE method allowed the comprehensive analyses of the Plasmodial proteome during its IDC. The recent report of the schizont stage *P. falciparum* proteome analyzed with 2-DE[8] prompted the analyses of expressed Plasmodial proteins during the ring and trophozoite stages of parasite development. Due to the just-in-time nature of transcript production per life cycle stage in the parasite, and little delay between transcript and protein production, the majority of this parasite's proteins are relatively life cycle specific[4]. Proteins are therefore expressed 0.75 to 1.5 times of a life cycle[3]. Highly synchronized parasites were used where proteins were isolated from either >98% pure ring stage or conversely trophozoite stage proteins. For the ring-stage parasite proteome, an average of 328 spots were detected on 2-DE with Flamingo Pink staining, and of these spots, 73 protein spots were identified by MS/MS. An average of 272 spots were detected on 2-DE with Flamingo Pink staining for the trophozoite proteome, of which 52 protein spots were positively identified by MS/MS, resulting in a total of 125 protein spots identified (out of 140 analyzed) in the late ring and trophozoite proteomes (Fig. 2, Table 2 A and B). These results confirmed the high MS success rate (90%) that was

achieved by applying the optimized methodology to the analyses of the Plasmodial proteome. The identified proteins all had significant MASCOT scores, at least 5 peptides identified, and sequence coverage of at least 10% each (Table 2 A and B). Of the 73 proteins spots identified in the ring stage proteome, 57 proteins spots were from Plasmodial origin, and consisted of 41 unique Plasmodial protein groups, where some groups contained multiple isoforms of the same protein. Therefore, protein isoforms represented 28% (16 isoforms) of the total number of Plasmodial protein spots identified. The trophozoite proteome consists of 52 protein spots identified by MS of which 49 protein spots were from Plasmodial origin. Of these, 29% (14 protein spots) accounted for isoforms from the 35 unique Plasmodial protein groups. From this data, it is clear that protein isoforms are prominent within both the ring and trophozoite stages and may play an important role in Plasmodial protein regulation. Similarly, this has also been demonstrated on 2-DE proteome maps for other protozoan parasites that also highlighted the importance of isoform detection and PTM's that regulate protein function[39-41]. The significance of isoforms is further exemplified in a 2-DE proteomic study of *T. brucei* where the absence of a single protein isoform was associated with drug resistance[42].

Comparison of the positively identified proteins groups from the ring (41 Plasmodial proteins) and trophozoite (35 Plasmodial proteins) stage proteomes to those of the schizont stage proteome (24 Plasmodial proteins)[8] revealed only 9 proteins (~9%) which were shared between all three stages. These include proteins involved in a variety of biological processes such as glycolysis, protein folding, oxidative stress and the cytoskeleton. Nineteen (19) proteins are shared between the ring and trophozoite stage whilst only 11 proteins were shared between the trophozoite and schizont. However, 14 proteins are shared between the ring and schizont stage parasites suggesting differentiation of the schizont stage proteins in preparation for the next round of invasion by the merozoites and the formation of the subsequent ring stage parasites. The remaining 39% of the proteins (39 proteins, 31 proteins from ring and trophozoite stage and 8 from schizont stage) were not shared between the different life stages

of the parasite, consistent with stage-specific production of proteins (and their transcripts) due to tightly controlled mechanisms within the parasite[3].

Comparison of the protein levels from the ring and trophozoite proteomes to the IDC transcript profile demonstrated distinct similarities between transcript production profiles (obtained from PlasmoDB 6.0 www.plasmodb.org)[28] and protein levels (Table 2A-B). Proteins that were up-regulated from rings to trophozoites mostly exhibited a corresponding increase in transcript level when compared to IDC data (Fig. 3, Table 2). Enolase, S-adenosylmethionine synthase, ornithine aminotransferase, uridine phosphorylase and disulfide isomerase all demonstrated an increase in abundance of both the transcript and protein expression levels. Similarly, eIF4A-like helicase and ribosomal phosphoprotein P0 all exhibited unchanged transcript and protein expression levels from ring to trophozoite stage parasites. These results emphasize the general observation of correspondences between transcript and protein levels in *P. falciparum*[4]. Actin-1 was one of the few exceptions in which transcript levels remained constant from ring to trophozoite stage parasites whilst protein levels were increasing. Similarly, the transcript levels of 2-Cys peroxiredoxin remained constant over the two time points whilst the protein was down-regulated. This could indicate possible differential regulation of these proteins at a post-transcriptional/translational level.

Of the 19 identified Plasmodial proteins shared between the ring and trophozoite stages of the parasite, several proteins appear as isoforms (Fig 4, isoforms are also marked in Fig 2 and Table 2 A-B). Moreover, some of these protein isoforms display differential regulation from the ring to trophozoite stages (Fig. 4). An increase in both transcript as well as protein expression levels were determined for the four enolase and phosphoethanolamine methyltransferase isoforms and the three glyceraldehyde-3-phosphate dehydrogenase isoforms. The transcript levels of pyruvate kinase (2 isoforms) increased over the specified period, but the protein expression levels for both isoforms declined. The transcript levels

for both triosephosphate isomerase (2 isoforms) and eIF4A (2 isoforms) remained constant during this period but the corresponding proteins increased in abundance. For glutamate dehydrogenase (3 isoforms) the transcript level decreased but the protein level remained constant from the ring to the trophozoite stages. Unchanged transcript and protein levels were detected for eIF4A-like helicase (2 isoforms). These examples demonstrate the complexity of post-transcriptional and post-translational regulation in the *P. falciparum* proteome.

Post-translational modification of proteins in *P. falciparum* has also been observed in the schizont stage proteome[8] similar to what has been detected within this study. Post-translational modifications of Plasmodial proteins include at least phosphorylation[43, 44], glycosylation[45-48], acetylation[49] and sulfonation[50]. The lateral shift of the eIF4A-like helicase isoforms in this study suggests phosphorylation or sulfonation as potential modifications (Fig. 3)[51, 52]. However, only 2 isoforms of this protein were observed in the trophozoite stage compared to 5 in the schizont stage, indicating additional regulatory mechanisms e.g. increased phosphorylation in later stages of the parasite[44] consistent with the proposed involvement of this protein in controlling developmentally regulated protein expression. Enolase seems to undergo post-translational modifications to produce 5 isoforms in *P. yoelii*, 7 isoforms in the *P. falciparum* schizont stages[8, 43] and 4 isoforms as described here. However, enolase phosphorylation was not reported in the *P. falciparum* phospho-proteome[44]. Some of these enolase-isoforms have also been detected in nuclei and membranes in *P. yoelii* and therefore suggests moonlighting functions including host cell invasion, stage-specific gene expression (*Toxoplasma*), stress responses and molecular chaperone functions[43]. The biological significance of these isoforms is not yet fully understood, but it clearly emphasizes the need for further in-depth investigations of post-transcriptional and post-translational modifications to further our understanding of the biological regulatory mechanisms within the Plasmodial parasite.

Concluding remarks

This is the first Plasmodial proteome study in which the 2-DE proteomic process was optimized in detail, from sample preparation through spot identification with MS/MS. This resulted in a more detailed description of the Plasmodial proteome due to the removal of contaminating hemoglobin without additional fractionation steps or extraction procedures. The fluorescent stain, Flamingo Pink, proved superior to the other stains tested and resulted in the detection of 79% of the predicted trophozoite proteome after 2-DE and achieved exceptional protein identification by MS. The reproducibility of the methods described here makes it highly expedient for the analysis of differentially expressed Plasmodial proteins. The application of the optimized 2-DE method allowed the characterization of 2-DE proteomes of the ring and trophozoite stages of *P. falciparum*, which showed that some proteins are differentially regulated between these life cycle stages and included the identification of a significant number of protein isoforms. Further analysis of the remainder of the detected spots is ongoing. These results emphasize the importance of post-translational modifications as regulatory mechanisms within this parasite.

Acknowledgements

Funding was provided by the National Research Foundation (NRF Grant FA2004051300055, Thuthuka TTK2006061500031 and Prestigious Bursary to SS), the South African Malaria Initiative (www.sami.org.za) and the University of Pretoria. Any opinions, findings and conclusions expressed in this paper are those of the authors.

SUPPORTING INFORMATION PARAGRAPH

Supplementary table 1A. List of proteins identified by MS/MS for Colloidal Coomassie Blue

Supplementary table 1B. List of proteins identified by MS/MS for MS-compatible silver stain

Supplementary table 1C. List of proteins identified by MS/MS for SYPRO Ruby

Supplementary table 1D. List of proteins identified by MS/MS for Flamingo Pink

This information is available free of charge via the internet at http://pubs.acs.org

FIGURE CAPTIONS

Figure 1. Comparison of Plasmodial proteins on 2-DE gels using four different stains.

Two-hundred micrograms of *Pf*3D7 proteins were loaded onto 13 cm IPG pH 3-10L strips for 2-DE analysis. After electrophoresis, the gels were stained with (A) Colloidal Coomassie Blue, (B) MS compatible silver stain, (C) SYPRO Ruby, (D) Flamingo Pink. The number of spots was determined using PD Quest 7.1.1 with n = 2 for each individual stain. About 39 similar spots were cut from each of the stained gels to determine the MS efficiency. The spots that were identified are marked on the gels.

Figure 2. 2-DE of the rings and trophozoites stage *P. falciparum* indicating identified proteins.

2-DE of Plasmodial ring-stage proteome (A) and its master image (C) compared to the 2-DE of early trophozoites stage proteome (B) and its corresponding master image (D). Master images were created by PD Quest as representative of all the 2-DE gels performed for each of the time points and contains spot information of a total of eight 2-DE gels. Plasmodial proteins are marked in white, human proteins are marked in yellow and bovine proteins are marked in red. Isoforms are encircled with dotted lines. The representing master images are also marked with identified proteins and all positively identified proteins are listed in Table 1 A and B.

Figure 3. Proteins that are differentially regulated in the *P. falciparum* ring and trophozoite stage proteomes.

Increased abundance is indicative of an increase in the abundance of the protein from ring to trophozoite stage, while unchanged is indicative of proteins that did not change in abundance and decreased abundance is indicative of a decrease in protein expression levels from the ring to the trophozoite stages.

MAT: S-adenosylmethionine synthase, OAT: ornithine aminotransferase

Figure 4. Isoforms of proteins that are differentially regulated in the *P. falciparum* ring and trophozoite stage proteomes.

The numbers are indicative of the number of isoforms per protein that were detected. Enolase, PEMT, and G3PDH, TIM and eIF4A all increase in protein abundance from the ring to the trophozoite stage. Pyruvate kinase decreased in protein abundance from rings to trophozoites, while glutamate dehydrogenase and eIF4A-like helicase remained unchanged over the specified time in protein expression levels. PEMT: phosphoethanolamine methyltransferase, TIM: triosephosphate isomerase, G3PDH: glyceraldehyde-3-phosphate dehydrogenase.

TABLES

Table 1. Comparative stain analysis for Plasmodial proteins analysed with 1-D as well as 2-DE SDS PAGE. Spot detection and MS identification rates are included for each of the four different stains, analysed on duplicate gels each (n=2).

1-D SDS PAGE MW analysis of stains			2-DE trophozoite analysis of stains			
Stain	LOD (ng)	R^2	Spots detected (PD Quest)	Nr cut for MS	Nr identified by MS	Identification success rate (%)
CCB	25-90	0.89	126	37	35	95
Silver	10-90	0.83	420	39	33	85
SYPRO	1-90	0.97	235	39	33	85
Flamingo	1-90	0.97	349	39	37	95
Total			1130	154	138	90[a]

[a] =average

Table 2 A. List of proteins identified by tandem mass spectrometry for late rings.

Spot nr[a]	Transcript trend[b]	PlasmoDB ID	Name	Mr (obtained) Da	pI (PlasmoDB)	Mascot Score MS/MS[c]	Seq Cover[d]	Match[e]
60	Up	PF10_0111	20S proteasome beta subunit, putative	30862	5.18	150	9	4
59	↔	PF14_0368	2-Cys peroxiredoxin	21964	6.65	540	59	8
46	↔	PF10_0264	40S ribosomal protein, putative (1)	30008	5.91	152	11	3
72	↔	PF10_0264	40S ribosomal protein, putative (2)	30008	5.91	146	14	4
35	↔	PFL2215w	Actin-I	42022	5.27	627	33	10
40	Up	PF10_0289	Adenosine deaminase, putative	42895	5.41	573	38	15
29	—	—	Bisphosphoglycerate mutase *(Homo sapiens)*	30027	6.1	441	46	10
53	—	—	Carbonic anhydrase 1 *(Homo sapiens)*	28778	6.63	531	50	8
54	—	—	Carbonic anhydrase 1 *(Homo sapiens)*	28620	6.65	845	58	11
55	—	—	Carbonic anhydrase 2 *(Homo sapiens)*	28802	6.63	320	30	7
16	—	—	Catalase *(Homo sapiens)*	59816	6.95	659	29	15
28	—	—	Catalase *(Homo sapiens)*	59816	6.95	425	22	9
15	Up	MAL8P1.17	Disulfide isomerase, putative (1)	55808	5.56	693	35	15
20	Up	MAL8P1.17	Disulfide isomerase, putative (2)	55808	5.56	1005	41	17
6	—	—	dnaK-type molecular chaperone hsc70 *(Bos*	71454	5.37	579	20	11
24	—	PF14_0655	eIF4A	45624	5.48	580	36	16
11	↔	PFB0445c	eIF4A-like helicase, putative (1)	52647	5.68	589	26	10
12	↔	PFB0445c	eIF4A-like helicase, putative (2)	52647	5.68	251	13	6
37	Up	PF11_0098	Endoplasmic reticulum-resident calcium binding	39464	4.49	1135	59	17
4	Up	PFL1070c	Endoplasmin homolog, putative	95301	5.28	298	14	10
22	Up	PF10_0155	Enolase (1)	48989	6.21	313	18	7
23	Up	PF10_0155	Enolase (2)	48989	6.21	373	18	7
25	Up	PF10_0155	Enolase (3)	48989	6.21	414	27	11
26	Up	PF10_0155	Enolase (4)	48989	6.21	1000	40	16
71	↔	PFL0210c	Eukaryotic initiation factor 5a, putative	17791	5.42	159	27	4
43	↔	PF14_0678	Exported protein 2	33619	5.1	379	26	8
44	↔	PF11_0165	Falcipain 2	56405	7.12	212	12	6
30	Down	PF14_0164	Glutamate dehydrogenase (NADP+) (1)	53140	7.48	283	17	8
31	Down	PF14_0164	Glutamate dehydrogenase (NADP+) (2)	53140	7.48	212	15	6

32	Down	PF14_0164	Glutamate dehydrogenase (NADP+) (3)	53140	7.48	497	30	13
61	—	PF14_0187	Glutathione s-transferase	24888	5.97	47	11	2
49	Up	PF14_0598	Glyceraldehyde-3-phosphate dehydrogenase (1)	37068	7.59	302	25	7
50	Up	PF14_0598	Glyceraldehyde-3-phosphate dehydrogenase (2)	37068	7.59	131	11	3
51	Up	PF14_0598	Glyceraldehyde-3-phosphate dehydrogenase (3)	37068	7.59	810	47	14
56	—	PF11_0183	GTP binding nuclear protein Ran	24974	7.72	485	55	12
41	Down	PF14_0078	HAP protein	51889	8.05	645	34	13
5	↔	PF08_0054	Heat shock 70 kDa protein	74382	5.51	1378	34	23
3	↔	PF07_0029	Heat shock protein 86	86468	4.94	1153	25	24
58	—	—	Hemoglobin subunit beta *(Homo sapiens)*	16112	6.75	294	43	6
10	Up	PF10_0153	Heat shock protein 60 kDa	62911	6.71	870	37	19
13	↔	PF14_0439	Leucine aminopeptidase, putative	68343	8.78	172	14	7
52	↔	PF13_0141	Lactate dehydrogenase	34314	7.12	611	43	12
14	↔	MAL13P1.283	MAL13P1.283 protein	58506	6.09	261	10	6
17	↔	PFE0585c	Myo-inositol 1-phosphate synthase, putative	69639	7.11	454	25	14
36	Down	PFL0185c	Nucleosome assembly protein 1, putative	42199	4.19	293	16	7
34	Up	PFF0435w	Ornithine aminotransferase	46938	6.47	589	27	11
68	—	—	Peroxiredoxin-2 *(Homo sapiens)*	21918	5.67	515	41	10
69	—	—	Peroxiredoxin-2 *(Homo sapiens)*	21918	5.67	664	43	11
64	Up	MAL13P1.214	Phosphoethanolamine N-methyltransferase,	31309	5.43	871	50	14
65	Up	MAL13P1.214	Phosphoethanolamine N-methyltransferase,	31309	5.43	935	50	14
66	Up	MAL13P1.214	Phosphoethanolamine N-methyltransferase,	31309	5.43	252	22	5
33	Up	PFI1105w	Phosphoglycerate kinase	45569	7.63	214	15	5
42	↔	PF14_0077	Plasmepsin 2	51847	5.35	72	6	3
48	↔	MAL8P1.142	Proteasome beta-subunit	31080	6.00	212	22	7
2	—	PFF0940c	Putative cell division cycle protein 48 homologue,	90690	4.95	303	10	7
18	Up	PFF1300w	Putative pyruvate kinase (1)	56480	7.50	633	28	15
19	Up	PFF1300w	Putative pyruvate kinase (2)	56480	7.50	732	37	16
67	—	PFI1270w	Putative uncharacterized protein PFI1270w	24911	5.49	327	26	6
47	↔	PF11_0313	Ribosomal phosphoprotein P0	35002	6.28	430	36	9
27	Up	PFI1090w	S-adenosylmethionine synthetase	45272	6.28	863	40	14
21	—	—	Selenium binding protein 1 *(Homo sapiens)*	52928	5.93	140	12	6
7	—	—	Serum albumin *(Bos Taurus)*	71274	5.82	620	24	15
57	—	—	Serum albumin *(Bos Taurus)*	71274	5.82	510	16	10
38	—	—	Solute carrier family 4, anion exchanger, member 1	101987	5.13	189	7	4

1	—	—	Spectrin alpha chain *(Homo sapiens)*	282024	4.98	889	24	9
70	—	—	Superoxide dismutase *(Homo sapiens)*	16154	5.70	219	37	4
39	↔	PFI0645w	Translation elongation factor 1 beta	32121	4.94	208	24	7
62	↔	PF14_0378	Triosephosphate isomerase (1)	27971	6.02	490	43	10
63	↔	PF14_0378	Triosephosphate isomerase (2)	27971	6.02	430	38	9
45	Up	PFE0660c	Uridine phosphorylase, putative (1)	27525	6.07	315	31	8
63	Up	PFE0660c	Uridine phosphorylase, putative (2)	27525	6.07	572	35	10
8	—	PF13_0065	V-type proton ATPase catalytic subunit A (1)	69160	5.51	291	19	10
9	—	PF13_0065	V-type proton ATPase catalytic subunit A (2)	69160	5.51	184	13	7

Table 2 B. List of proteins identified by tandem mass spectrometry for early trophozoites.

Spot nr[a]	Transcript trend[b]	PlasmoDB ID	Name	Mr (obtained) Da	pI (PlasmoDB)	Mascot Score MS/MS[c]	Seq Cover[d]	Match[e]
50	↔	PF14_0368	2-Cys peroxiredoxin	21964	6.65	504	72	11
45	Down	PFC0295c	40S ribosomal protein S12, putative (1)	15558	4.67	85	14	2
47	Down	PFC0295c	40S ribosomal protein S12, putative (2)	15558	4.67	217	36	5
28	↔	PF10_0264	40S ribosomal protein, putative (1)	30008	5.91	27	11	3
29	↔	PF10_0264	40S ribosomal protein, putative (2)	30008	5.91	267	24	8
40	Up	PF14_0036	Acid phosphatase, putative	35972	6.3	63	5	2
51	↔	PFL2215w	Actin-1 (1)	42272	5.17	81	36	12
16	↔	PFL2215w	Actin-1 (2)	42022	5.27	455	36	9
38	↔	PFL2215w	Actin-1 (3)	42022	5.27	225	14	5
48	—	—	Carbonic anhydrase 1 *(Homo sapiens)*	28620	6.65	70	20	4
15	Up	MAL8P1.17	Disulfide isomerase precursor, putative	55808	5.56	883	38	16
18	Up	PF14_0655	eIF4A (1)	45624	5.28	353	30	12
19	Up	PF14_0655	eIF4A (2)	45624	5.48	326	23	12
13	↔	PFB0445c	eIF4A-like helicase, putative (1)	52647	5.68	320	23	8
14	↔	PFB0445c	eIF4A-like helicase, putative (2)	52646	5.68	62	42	14
5	↔	PF14_0486	Elongation factor 2 (1)	94546	6.36	91	4	4
6	↔	PF14_0486	Elongation factor 2 (2)	94546	6.78	657	26	18
20	↔	PF10_0155	Enolase (1)	48989	6.21	408	32	10
21	↔	PF10_0155	Enolase (2)	48989	6.21	949	36	12
30	—	PFD0615c	Eryhrocyte membrane protein 1 (fragment)	13608	6.96	51	38	7
33	↔	PF11_0165	Falcipain 2 (1)	56481	7.9	47	23	10
34	↔	PF11_0165	Falcipain 2 (2)	55928	7.49	56	24	11
11	↔	PF14_0341	Glucose-6-phosphate isomerase	67610	6.78	61	28	14
24	Down	PF14_0164	Glutamate dehydrogenase (NADP+)	53140	7.48	336	28	11
39	↔	PF10_0325	Haloacid dehalogenase-like hydrolase, putative	33220	5.62	180	27	6
7	↔	PF08_0054	Heat shock 70 kDa protein	74382	5.33	861	33	18
52	Up	PF10_0153	Heat shock protein 60 kDa	62911	6.71	128	38	21
35	Up	PF11_0069	Hypothetical protein	32112	4.91	55	13	3
36	Up	PF14_0138	Hypothetical protein	23889	5.49	53	9	2

23	Up	MAL13P1.23	Hypothetical protein MAL13P1.237	42475	7.14	574	37	13
17	Down	MAL8P1.95	Hypothetical protein MAL8P1.95	37933	4.13	385	25	8
10	↔	PF14_0324	Hypothetical protein, conserved	66415	6.63	66	7	4
25	Up	PF13_0141	Lactate dehydrogenase	34314	7.12	100	12	3
1	↔	MAL13P1.56	M1 family aminopeptidase (1)	126552	7.3	102	26	23
2	↔	MAL13P1.56	M1 family aminopeptidase (2)	126552	6.68	124	26	25
3	↔	MAL13P1.56	M1 family aminopeptidase (3)	126552	7.3	107	27	23
22	Up	PFF0435w	Ornithine aminotransferase	46938	6.47	637	29	12
37	Up	MAL13P1.21	Phosphoethanolamine N-methyltransferase,	31043	5.28	69	9	2
38	Up	MAL13P1.21	Phosphoethanolamine N-methyltransferase,	31043	5.28	261	26	6
41	Up	MAL13P1.21	Phosphoethanolamine N-methyltransferase,	31309	5.28	177	22	5
42	Up	MAL13P1.21	Phosphoethanolamine N-methyltransferase,	31309	5.28	722	48	13
49	↔	PF11_0208	Phosphoglycerate mutase, putative	28866	8.3	401	36	10
26	Down	PF14_0076	Plasmepsin-1	51656	6.72	540	35	12
43	↔	PF14_0716	Proteosome subunit alpha type 1, putative	29218	5.51	268	31	6
46	—	PFL0590c	P-type ATPase, putative	135214	6.13	54	18	16
12	Up	PFF1300w	Putative pyruvate kinase	56480	7.5	101	51	16
31	↔	PF11_0313	Ribosomal phosphoprotein P0	35002	6.28	121	13	3
22	Up	PFI1090w	S-adenosylmethionine synthetase	45272	6.28	480	32	10
8	—	—	Serum albumin *(Bos Taurus)*	71274	5.82	466	24	15
9	—	—	Serum albumin *(Bos Taurus)*	71274	5.82	822	36	21
27	↔	PFI0645w	Translation elongation factor 1 beta	32121	4.94	488	35	9
44	Up	PF14_0378	Triosephosphate isomerase	27971	6.02	183	22	6

Proteins identified are sorted alphabetically according to name with isoforms grouped together and the number of isoforms per protein is marked in brackets.

[a]Spot number corresponds to marked spots on the master image of ring stage parasites.

[b]Trend of transcripts regulation from 16-20 HPI as acquired from the IDC database (http://malaria.ucsf.edu/comparison/index.php) for each of the identified proteins. (↔) indicates unchanged transcript levels and (—) is indicative that result is not applicable.

[c]Mascot scores are based on MS/MS searches and is only taken when the score is significant ($p<0.05$).

[d]Sequence coverage is given by Mascot for detected peptide sequences.

[e]Matched is the number of peptides matched to the particular protein

References

1. Noedl, H.; Se, Y.; Schaecher, K.; Smith, B. L.; Socheat, D.; Fukuda, M. M. Evidence of Artemisinin-Resistant Malaria in Western Cambodia. *New Engl. J. Med.* **2008,** 359 (24), 2619-2620.

2. Birkholtz, L.; van Brummelen, A. C.; Clark, K.; Niemand, J.; Marechal, E.; Llinas, M.; Louw, A. I. Exploring functional genomics for drug target and therapeutics discovery in Plasmodia. *Acta Trop.* **2008,** 105 (2), 113-123.

3. Bozdech, Z.; Llinas, M.; Pulliam, B. L.; Wong, E. D.; Zhu, J. C.; DeRisi, J. L. The transcriptome of the intraerythrocytic developmental cycle of *Plasmodium falciparum*. *PLoS Biol.* **2003,** 1 (1), 85-100.

4. Le Roch, K. G.; Johnson, J. R.; Florens, L.; Zhou, Y. Y.; Santrosyan, A.; Grainger, M.; Yan, S. F.; Williamson, K. C.; Holder, A. A.; Carucci, D. J.; Yates, J. R.; Winzeler, E. A. Global analysis of transcript and protein levels across the *Plasmodium falciparum* life cycle. *Genome Res.* **2004,** 14 (11), 2308-2318.

5. Shock, J. L.; Fischer, K. F.; DeRisi, J. L. Whole-genome analysis of mRNA decay in *Plasmodium falciparum* reveals a global lengthening of mRNA half-life during the intra-erythrocytic development cycle. *Genome Biol.* **2007,** 8 (7).

6. Sims, P. F. G.; Hyde, J. E. Proteomics of the human malaria parasite *Plasmodium falciparum*. *Expert Rev. Proteomics* **2006,** 3 (1), 87-95.

7. Nirmalan, N.; Sims, P. F. G.; Hyde, J. E. Quantitative proteomics of the human malaria parasite *Plasmodium falciparum* and its application to studies of development and inhibition. *Mol. Microbiol.* **2004,** 52 (4), 1187-1199.

8. Foth, B. J.; Zhang, N.; Mok, S.; Preiser, P. R.; Bozdech, Z. Quantitative protein expression profiling reveals extensive post-transcriptional regulation and post-translational modifications in schizont-stage malaria parasites. *Genome Biol.* **2008,** 9, R177.

9. Gardner M.J.; Hall N.; Fung E.; White O.; Berriman M.; Hyman R.W.; Carlton J.M.; Pain A.; Nelson K.E.; Bowman S.; Paulsen I.T.; James K.; Eisen J.A.; Rutherford K.; Salzberg S.L.; Craig A.; Kyes S.; Chan M.S.; Nene V.; Shallom S.J.; Suh B.; Peterson J.; Angiuoli S.; Pertea M.; Allen J.; Selengut J.; Haft D.; Mather M.W.; Vaidya A.B.; Martin D.M.A.; Fairlamb A.H.; Fraunholz M.J.; Roos D.S.; Ralph S.A.; McFadden G.I.; Cummings L.M.; Subramanian G.M.; Mungall C.; Venter J.C.; Carucci D.J.; Hoffman S.L.; Newbold C.; Davis R.W.; Fraser C.M.; Barrell B. Genome sequence of the human malaria parasite *Plasmodium falciparum*. *Nature* **2002,** 419, 498-511.

10. Birkholtz, L.; Blatch, G.; Coetzer, T.; Hoppe, H.; Human, E.; Morris, E.; Ngcete, Z.; Oldfield, L.; Roth, R.; Shonhai, A.; Stephens, L.; Louw, A. Heterologous expression of Plasmodial proteins for structural studies and functional annotation. *Malaria J.* **2008,** 7 (1), 197.

11. Mehlin, C.; Boni, E.; Buckner, F. S.; Engel, L.; Feist, T.; Gelb, M. H.; Haji, L.; Kim, D.; Liu, C.; Mueller, N.; Myler, P. J.; Reddy, J. T.; Sampson, J. N.; Subramanian, E.; Van Voorhis, W. C.; Worthey, E.; Zucker, F.; Hol, W. G. J. Heterologous expression of proteins from *Plasmodium falciparum*: Results from 1000 genes. *Mol. Biochem. Parasitol.* **2006,** 148 (2), 144-160.

12. Vedadi, M.; Lew, J.; Artz, J.; Amani, M.; Zhao, Y.; Dong, A. P.; Wasney, G. A.; Gao, M.; Hills, T.; Brokx, S.; Qiu, W.; Sharma, S.; Diassiti, A.; Alam, Z.; Melone, M.; Mulichak, A.; Wernimont, A.; Bray, J.; Loppnau, P.; Plotnikova, O.; Newberry, K.; Sundararajan, E.; Houston, S.; Walker, J.; Tempel, W.; Bochkarev, A.; Kozieradzki, L.; Edwards, A.; Arrowsmith, C.; Roos, D.; Kain, K.; Hui, R. Genome-scale protein expression and structural biology of *Plasmodium falciparum* and related Apicomplexan organisms. *Mol. Biochem. Parasitol.* **2007,** 151 (1), 100-110.

13. Gelhaus, C.; Fritsch, J.; Krause, E.; Leippe, M. Fractionation and identification of proteins by 2DE and MS: towards a proteomic analysis of *Plasmodium falciparum*. *Proteomics* **2005,** 5.

14. Makanga, M.; Bray, P. G.; Horrocks, P.; Ward, S. A. Towards a proteomic definition of CoArtem action in *Plasmodium falciparum* malaria. *Proteomics* **2005,** 5, 1-10.

15. Panpumthong, P.; Vattanaviboon, P. Improvement of proteomic profile of *Plasmodium falciparum* by two step protein extraction in two dimensional gel electrophoresis. *Thammasat Int. J. Sc. Tech.* **2006,** 11 (3), 61-68.

16. Radfar, A.; Diez, A.; Bautista, J. M. Chloroquine mediates specific proteome oxidative damage across the erythrocytic cycle of resistant *Plasmodium falciparum*. *Free Radical Biol. Med.* **2008,** 44 (12), 2034-2042.

17. Wu, Y.; Craig, A. Comparative proteomic analysis of metabolically labelled proteins from *Plasmodium falciparum* isolates with different adhesion properties. *Malaria J.* **2006,** 5, 67.

18. Trager, W.; Jensen, J. B. Human malaria parasites in continuous culture. *Science* **1976,** 193 (4254), 673-675.

19. Bradford, M. M. A rapid and sensitive method for the quantitation of microgram quantities of protein utilizing the principle of protein-dye binding. *Anal. Biochem.* **1976,** 72, 248-254.

20. Lowry, O. H.; Rosebrough, N. J.; Farr, A. L.; Randall, R. J. Protein measurement with the Folin Phenol Reagent. *J. Biol. Chem.* **1951,** 193, 265-275.

21. Neuhoff, V.; Arold, N.; Taube, D.; Ehrhardt, W. Improved staining of proteins in polyacrylamide gels including isoelectric focusing gels with clear background at nanogram sensitivity using Coomassie Brilliant Blue G-250 and R-250. *Electrophoresis* **1988,** 9, 255-262.

22. Gharahdaghi, F.; Weinberg, C. R.; Meagher, D. A.; Imai, B. S.; Mische, S. M. Mass spectrometric identification of proteins from silver-stained polyacrylamide gel: A method for the removal of silver ions to enhance sensitivity. *Electrophoresis* **1999,** 20 (3), 601-605.

23. Wang, P.; Bouwman, F. G.; Mariman, E. C. M. Generally detected proteins in comparative proteomics – A matter of cellular stress response? *Proteomics* **2009,** 9, 1-12.

24. Lopez, M. F. Better approaches to finding the needle in a haystack: Optimizing proteome analysis through automation. *Electrophoresis* **2000,** 21, 1082-1093.

25. Ong, S. E.; Pandey, A. An evaluation of the use of two-dimensional gel electrophoresis in proteomics. *Biomol. Eng.* **2001,** 18 (5), 195-205.

26. van Brummelen, A. C.; Olszewski, K. L.; Wilinski, D.; Llinás, M.; Louw, A. I.; Birkholtz, L. Co-inhibition of *Plasmodium falciparum* S-Adenosylmethionine Decarboxylase/Ornithine Decarboxylase Reveals Perturbation-specific Compensatory Mechanisms by Transcriptome, Proteome, and Metabolome Analyses. *J. Biol. Chem.* **2009,** 284 (7), 4635-4646.

27. Florens, L.; Washburn, M. P.; Raine, J. D.; Anthony, R. M.; Grainger, M.; Haynes, J. D.; Moch, J. K.; Muster, N.; Sacci, J. B.; Tabb, D. L.; Witney, A. A.; Wolters, D.; Wu, Y. M.; Gardner, M. J.; Holder, A. A.; Sinden, R. E.; Yates, J. R.; Carucci, D. J. A proteomic view of the *Plasmodium falciparum* life cycle. *Nature* **2002,** 419 (6906), 520-526.

28. Aurrecoechea, C.; Brestelli, J.; Brunk, B. P.; Dommer, J.; Fischer, S.; Gajria, B.; Gao, X.; Gingle, A.; Grant, G.; Harb, O. S.; Heiges, M.; Innamorato, F.; Iodice, J.; Kissinger, J. C.; Kraemer, E.; Li, W.; Miller, J. A.; Nayak, V.; Pennington, C.; Pinney, D. F.; Roos, D. S.; Ross, C.; Stoeckert Jr, C. J.; Treatman, C.; Wang, H. PlasmoDB: a functional genomic database for malaria parasites. *Nucleic Acids Res.* **2008,** 37 (January), D539-D543.

29. Berggren, K.; Chernokalskaya, E.; Steinberg, T. H.; Kemper, C.; Lopez, M. F.; Diwu, Z.; Haugland, R. P.; Patton, W. F. Background-free, high sensitivity staining of proteins in one- and two-dimensional sodium dodecyl sulfate-polyacrylamide gels using a luminescent ruthenium complex. *Electrophoresis* **2000,** 21 (12), 2509-2521.

30. Steinberg, T. H.; Jones, L. J.; Haugland, R. P.; Singer, V. L. SYPRO Orange and SYPRO Red gel stains: One-step fluorescent staining of denaturing gels for detection of nanogram levels of protein. *Anal. Biochem.* **1996,** 239, 223-237.

31. Steinberg, T. H.; Haugland, R. P.; Singer, V. L. Applications of SYPRO Orange and SYPRO Red protein gel stains. *Anal. Biochem.* **1996,** 239, 238-245.

32. Yan, J. X.; Harry, R. A.; Spibey, C.; Dunn, M. J. Postelectrophoretic staining of proteins separated by two-dimensional gel electrophoresis using SYPRO dyes. *Electrophoresis* **2000,** 21 (17), 3657-3665.

33. Lopez, M. F.; Berggren, K.; Chernokalskaya, E.; Lazarev, A.; Robinson, M.; Patton, W. F. A comparison of silver stain and SYPRO Ruby Protein Gel Stain with respect to protein detection in two-dimensional gels and identification by peptide mass profiling. *Electrophoresis* **2000,** 21 (17), 3673-3683.

34. Harris, L. R.; Churchward, M. A.; Butt, R. H.; Coorssen, J. R. Assessing detection methods for gel-based proteomic analyses. *J. Proteome Res.* **2007,** (6), 1418-1425.

35. Winkler, C.; Denker, K.; Wortelkamp, S.; Sickmann, A. Silver- and coomassie-staining protocols: Detection limits and compatibility with ESI MS. *Electrophoresis* **2007,** 28 (12), 2095-2099.

36. Lauber, W. M.; Carroll, J. A.; Dufield, D. R.; Kiesel, J. R.; Radabaugh, M. R.; Malone, J. P. Mass spectrometry compatibility of two-dimensional gel protein stains. *Electrophoresis* **2001,** 22 (5), 906-918.

37. Nirmalan, N.; Flett, F.; Skinner, T.; Hyde, J. E.; Sims, P. F. G. Microscale solution lsoelectric focusing as an effective strategy enabling containment of hemeoglobin-derived products for high-resolution gel-based analysis of the *Plasmodium falciparum* proteome. *J. Proteome Res.* **2007,** 6 (9), 3780-3787.

38. Aly, N. S. M.; Hiramoto, A.; Sanai, H.; Hiraoka, O.; Hiramoto, K.; Kataoka, H.; Wu, J. M.; Masuyama, A.; Nojima, M.; Kawai, S.; Kim, H. S.; Wataya, Y. Proteome analysis of new antimalarial endoperoxide against *Plasmodium falciparum*. *Parasitol. Res.* **2007**.

39. De Jesus, J. B.; Cuervo, P.; Junqueira, M.; Britto, C.; Silva-Filho, F. C.; Saboia-Vahia, L.; Gonzalez, L. J.; Domont, G. B. Application of two-dimensional electrophoresis and matrix-assisted laser desorption/ionization time-of-flight mass spectrometry for proteomic analysis of the sexually transmitted parasite *Trichomonas vaginalis*. *J. Mass Spectrom.* **2007,** 42 (11), 1463-1473.

40. Brobey, R. K. B.; Soong, L. Establishing a liquid-phase IEF in combination with 2-DE for the analysis of *Leishmania* proteins. *Proteomics* **2007,** 7 (1), 116-120.

41. Jones, A.; Faldas, A.; Foucher, A.; Hunt, E.; Tait, A.; Wastling, J. M.; Turner, C. M. Visualisation and analysis of proteomic data from the procyclic form of *Trypanosoma brucei. Proteomics* **2006,** 6 (1), 259-267.

42. Foucher, A. L.; McIntosh, A.; Douce, G.; Wastling, J.; Tait, A.; Turner, C. M. R. A proteomic analysis of arsenical drug resistance in *Trypanosoma brucei*. *Proteomics* **2006,** 6 (9), 2726-2732.

43. Pal-Bhowmick, I.; Vora, H. K.; Jarori, G. K. Sub-cellular localization and post-translational modifications of the *Plasmodium yoelii* enolase suggest moonlighting functions. *Malaria J.* **2007,** 6.

44. Wu, Y.; Nelson, M. M.; Quaile, A.; Xia, D.; Wastling, J. M.; Craig, A. Identification of phosphorylated proteins in erythrocytes infected by the human malaria parasite *Plasmodium falciparum. Malaria J.* **2009,** 8.

45. Davidson, E. A.; Gowda, D. C.; Yang, S. T.; Nikodem, D.; Naik, R. Glycobiology of the malaria parasite. *Glycobiology* **1999,** 9 (10), 52.

46. Gowda, D. C.; Davidson, E. A. Protein glycosylation in the malaria parasite. *Parasitol. Today* **1999,** 15 (4), 147-152.

47. Yang, S. T.; Nikodem, D.; Davidson, E. A.; Gowda, D. C. Glycosylation and proteolytic processing of 70 kDa C-terminal recombinant polypeptides of *Plasmodium falciparum* merozoite surface protein 1 expressed in mammalian cells. *Glycobiology* **1999,** 9 (12), 1347-1356.

48. Davidson, E. A.; Gowda, D. C. Glycobiology of *Plasmodium falciparum*. *Biochimie* **2001,** 83 (7), 601-604.

49. Miao, J.; Fan, Q.; Cui, L.; Li, J. S.; Li, J. Y.; Cui, L. W. The malaria parasite *Plasmodium falciparum* histones: Organization, expression, and acetylation. *Gene* **2006,** 369, 53-65.

50. Medzihradszky, K. F.; Darula, Z.; Perlson, E.; Fainzilber, M.; Chalkley, R. J.; Ball, H.; Greenbaum, D.; Bogyo, M.; Tyson, D. R.; Bradshaw, R. A.; Burlingame, A. L. O-sulfonation of serine and threonine - Mass spectrometric detection and characterization of a new posttranslational modification in diverse proteins throughout the eukaryotes. *Mol. Cell. Proteomics* **2004,** 3 (5), 429-440.

51. Kinoshita, E.; Kinoshita-Kikutal, E.; Matsubara, M.; Aoki, Y.; Ohie, S.; Mouri, Y.; Koike, T. Two-dimensional phosphate-affinity gel electrophoresis for the analysis of phosphoprotein isotypes. *Electrophoresis* **2009,** 30 (3), 550-559.

52. Thingholm, T. E.; Jensen, O. N.; Larsen, M. R. Analytical strategies for phosphoproteomics. *Proteomics* **2009,** 9 (6), 1451-1468.

SYNOPSIS

An optimized 2-DE method was established that enabled the detection of a large number of the trophozoite proteome and achieved a 95% identification success rate by MS. Subsequently, this methodology was applied to the Plasmodial ring and trophozoite proteome that allowed the positive identification of 125 protein spots. The existence of various isoforms within the Plasmodial proteome were identified that may have significant biological importance within the Plasmodial parasite.

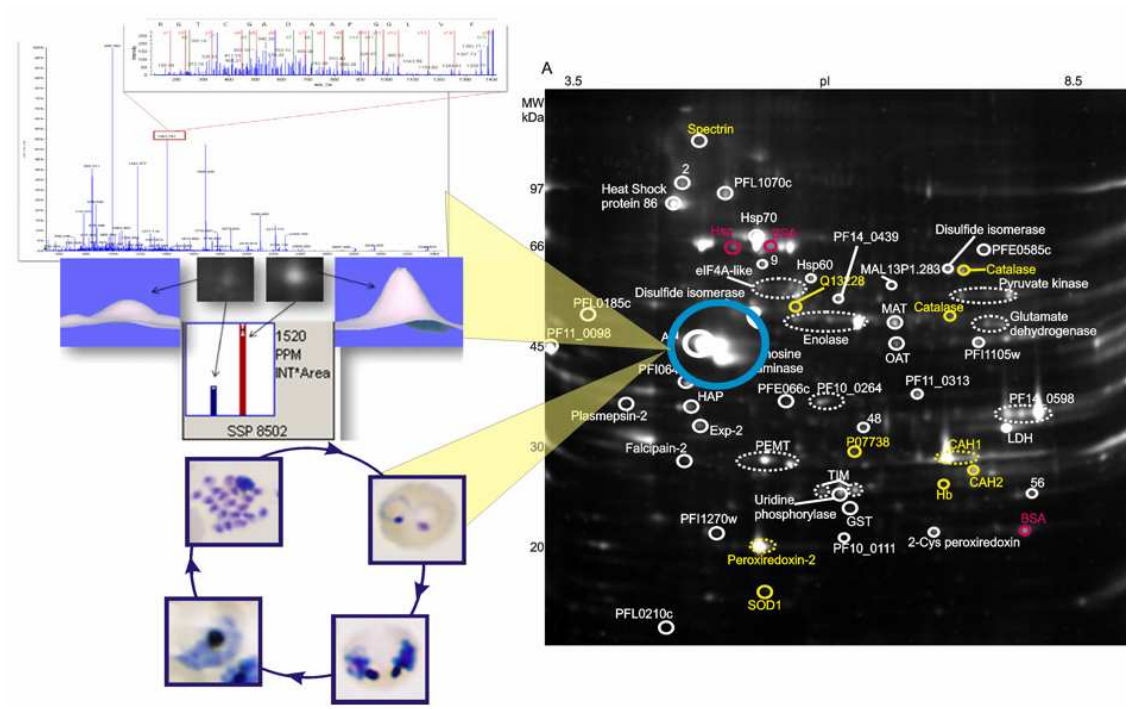

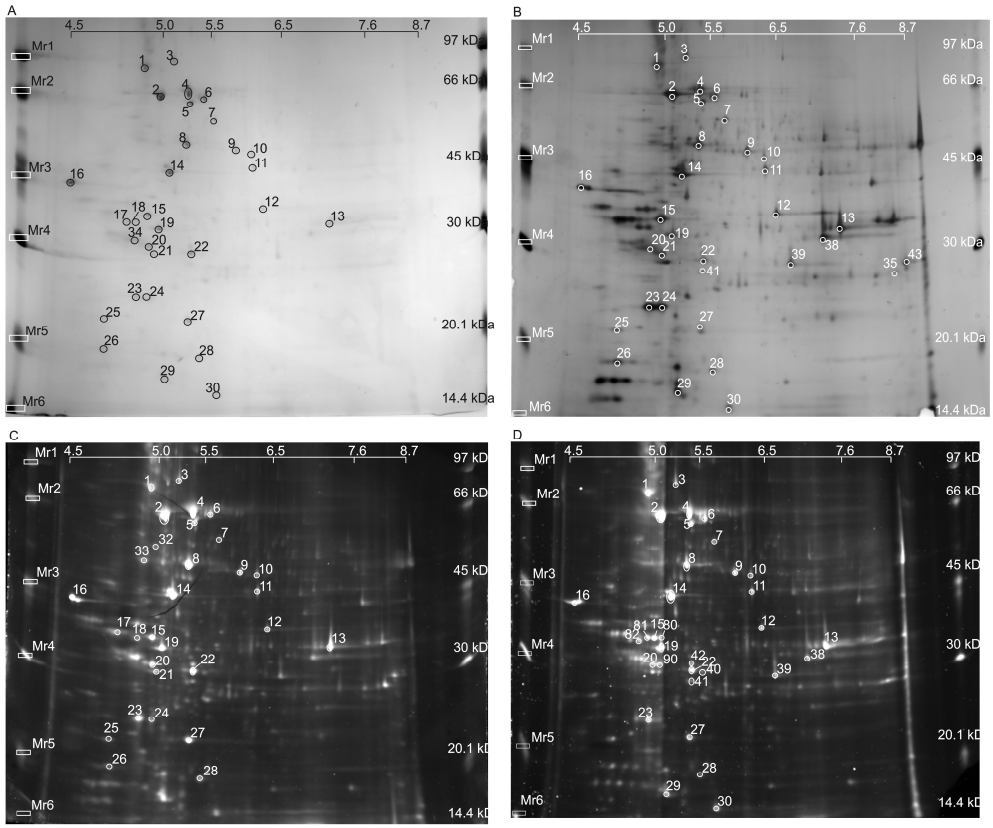

Figure 1. Comparison of Plasmodial proteins on 2-DE gels using four different stains. Two-hundred micrograms of Pf3D7 proteins were loaded onto 13 cm IPG pH 3-10L strips for 2-DE analysis. After electrophoresis, the gels were stained with (A) Colloidal Coomassie Blue, (B) MS compatible silver stain, (C) SYPRO Ruby, (D) Flamingo Pink. The number of spots was determined using PD Quest 7.1.1. About 39 similar spots were cut from each of the stained gels to determine the MS efficiency. The spots that were identified are marked on the gels.

178x148mm (600 x 600 DPI)

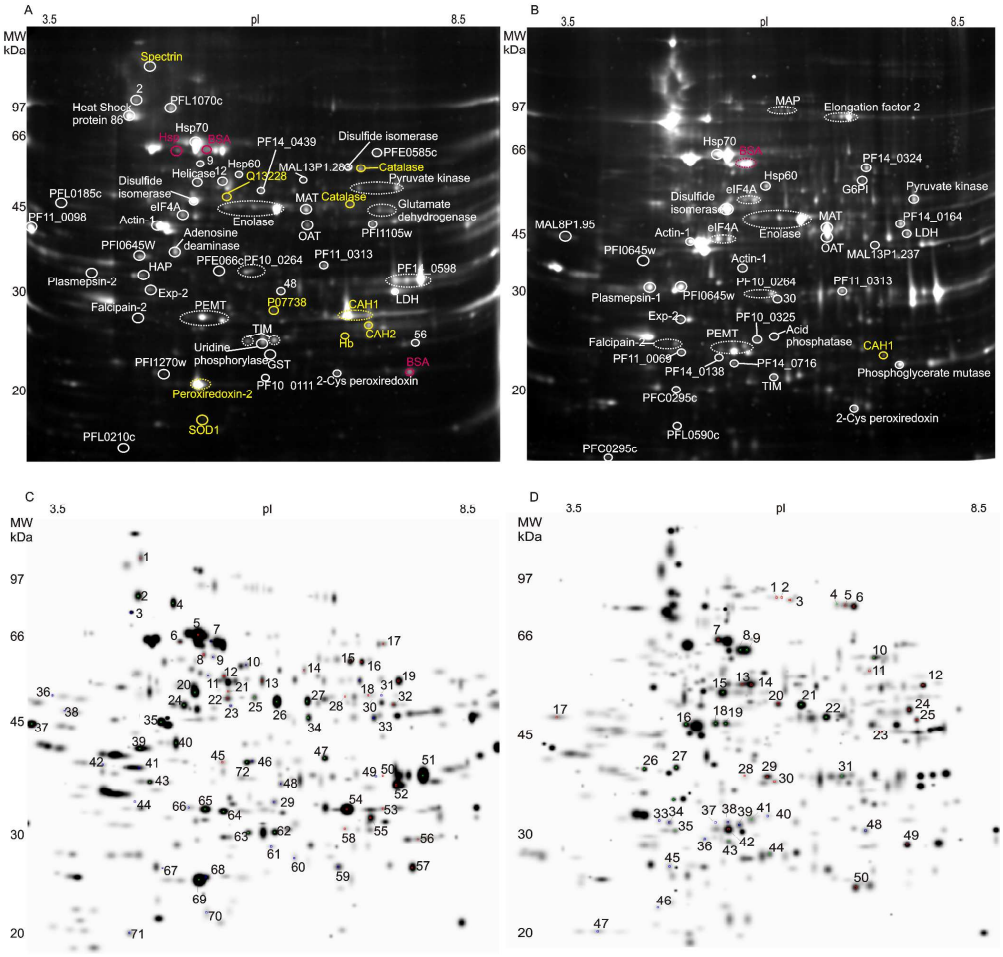

Figure 2. 2-DE of the rings and trophozoites stage P. falciparum indicating identified proteins. 2-DE of Plasmodial ring-stage proteome (A) and its master image (C) compared to the 2-DE of early trophozoites stage proteome (B) and its corresponding master image (D). Master images were created by PD Quest as representative of all the 2-DE gels performed for each of the time points and contains spot information of a total of eight 2-DE gels. Plasmodial proteins are marked in white, human proteins are marked in yellow and bovine proteins are marked in red. Isoforms are encircled with dotted lines. The representing master images are also marked with identified proteins and all positively identified proteins are listed in Table 1 A and B.

178x171mm (600 x 600 DPI)

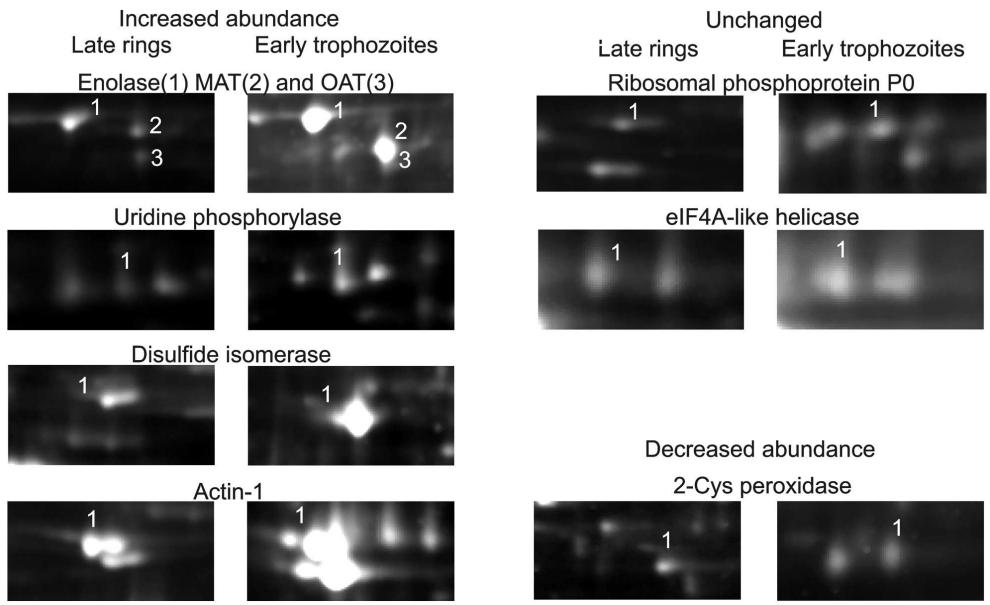

Figure 3. Proteins that are differentially regulated in the P. falciparum ring and trophozoite stage proteomes.
Increased abundance is indicative of an increase in the abundance of the protein from ring to trophozoite stage, while unchanged is indicative of proteins that did not change in abundance and decreased abundance is indicative of a decrease in protein expression levels from the ring to the trophozoite stages. MAT: S-adenosylmethionine synthase, OAT: ornithine aminotransferase

85x51mm (600 x 600 DPI)

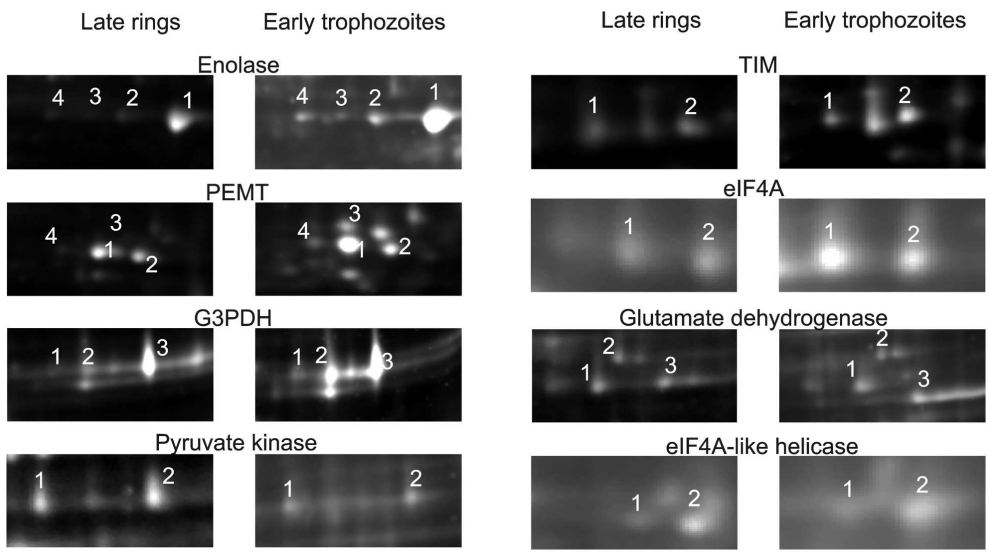

Figure 4. Isoforms of proteins that are differentially regulated in the P. falciparum ring and trophozoite stage proteomes.
The numbers are indicative of the number of isoforms per protein that were detected. Enolase, PEMT, and G3PDH, TIM and eIF4A all increase in protein abundance from the ring to the trophozoite stage. Pyruvate kinase decrease in protein abundance from rings to trophozoites, while glutamate dehydrogenase and eIF4A-like helicase remained unchanged over the specified time in protein expression levels. PEMT: phosphoethanolamine methyltransferase, TIM: triosephosphate isomerase, G3PDH: glyceraldehyde-3-phosphate dehydrogenase.

85x47mm (600 x 600 DPI)